SIAM J. SCI. COMPUT. © 2020 Society for Industrial and Applied Mathematics
Vol. 42, No. 2, pp. A1226–A1244

NUMERICAL APPROXIMATION OF OPTIMAL CONVEX SHAPES*

SÖREN BARTELS† AND GERD WACHSMUTH‡

Abstract. This article investigates the numerical approximation of shape optimization problems with PDE constraint on classes of convex domains. The convexity constraint provides a compactness property which implies well posedness of the problem. Moreover, we prove the convergence of discretizations in two-dimensional situations. A numerical algorithm is devised that iteratively solves the discrete formulation. Numerical experiments show that optimal convex shapes are generally nonsmooth and that three-dimensional problems require an appropriate relaxation of the convexity condition.

Key words. shape optimization, PDE constraints, convexity, convergence, iterative solution

AMS subject classifications. 49Q10, 65N12

DOI. 10.1137/19M1256853

1. Introduction.

Shape optimization has become a popular area of research in applied mathematics and is relevant in various technological applications. Existence theories and convergence results for numerical approximation methods often depend on appropriate regularizations, e.g., via a perimeter functional. In this paper we consider partial differential equation (PDE) constrained shape optimization problems that are restricted to classes of convex shapes. A convexity condition appears reasonable in many applications and may in some situations replace a more natural but mathematically more involved connectedness restriction. Imposing constraints on sets of admissible shapes is often necessary to guarantee the existence of a solution; cf., e.g., Bucur et al. (2017); Bartels and Buttazzo (2018) for a problem occurring in optimal insulation.

We consider a model PDE constrained shape optimization problem with convexity constraint which reads as follows:

$$\textbf{(P)} \qquad \begin{aligned} &\text{Minimize} && \int_\Omega j(x, u(x), \nabla u(x))\,\mathrm{d}x \\ &\text{w.r.t.} && \Omega \subset \mathbb{R}^d,\ u \in H_0^1(\Omega), \\ &\text{s.t.} && -\Delta u = f \text{ in } \Omega \text{ and } \Omega \subset Q \text{ convex and open.} \end{aligned}$$

Here, $Q \subset \mathbb{R}^d$ is a bounded, convex, and open hold-all domain, $j : Q \times \mathbb{R} \times \mathbb{R}^d \to \mathbb{R}$ is a suitable Carathéodory function, and the right-hand side in the state equation is assumed to satisfy $f \in L^2(Q)$. We stress that the quantity of interest is the a priori unknown shape Ω. Particular attention in this article is paid to the convexity constraint, which enables us to prove existence of solutions and convergence of approximations but which also leads to difficulties in its appropriate numerical treatment. After

*Submitted to the journal's Methods and Algorithms for Scientific Computing section April 17, 2019; accepted for publication (in revised form) February 14, 2020; published electronically April 22, 2020.
https://doi.org/10.1137/19M1256853
Funding: This work was supported by the DFG through grants within the Priority Program SPP 1962 (Non-smooth and Complementarity-based Distributed Parameter Systems: Simulation and Hierarchical Optimization).

†Department of Applied Mathematics, Albert-Ludwigs-Universität Freiburg, 79104 Freiburg i.Br., Germany (bartels@mathematik.uni-freiburg.de, https://aam.uni-freiburg.de/agba).
‡Institute of Mathematics, Brandenburgische Technische Universität Cottbus-Senftenberg, 03046 Cottbus, Germany (gerd.wachsmuth@b-tu.de, https://www.b-tu.de/fg-optimale-steuerung).

establishing existence of solutions under suitable assumptions on the function j, we prove convergence of numerical approximation schemes for two-dimensional problems. We then devise an iterative scheme for computing optimal shapes and discuss numerical experiments which reveal that optimal convex shapes are typically nonsmooth and that the convexity constraint has to be relaxed in three-dimensional situations.

There are very few references discussing existence results for shape optimization problems with convexity constraints. To the best of our knowledge, the first one is Buttazzo and Guasoni (1997), where the authors study the minimization of certain geometric functionals defined via

$$F(\Omega) = \int_{\partial\Omega} j(x, \nu(x))\,\mathrm{d}\mathcal{H}^{d-1}.$$

Here, $\mathcal{H}^{d-1}$ is the $(d-1)$-dimensional Hausdorff measure and $\nu(x)$ is the (outer) normal vector of Ω at x (which exists $\mathcal{H}^{d-1}$-a.e. on $\partial\Omega$). Existence results for shape optimization problems involving convexity and PDE constraints are given in Van Goethem (2004); Yang (2009). In the former contribution, linear elliptic PDEs of even order are considered, and the latter reference addresses the situation of the stationary Navier–Stokes equation under a smallness assumption on the data. None of these articles addresses the practical solution of the problems.

Another interesting result concerning convex shape optimization is provided in Bucur (2003), in which regularity of optimal convex shapes for a class of objectives is proved. In particular, the author considers problem (**P**) with the objective

$$\int_Q j(x, u(x))\,\mathrm{d}x + \alpha \int_\Omega 1\,\mathrm{d}x$$

for some positive regularization parameter $\alpha > 0$. Note that the first integral ranges over the hold-all domain Q, and u is extended by 0 outside of Ω. It is shown that the optimal shape has a C^1 boundary under some weak assumptions, namely it is required that j is Lipschitz continuous in its second argument and that $f \in L^\infty(Q)$. Under these conditions the objective value can be decreased by rounding corners. However, the arguments do not apply to the case of a vanishing regularization parameter $\alpha = 0$ or if j is integrated only over Ω, which is the situation considered in this article.

To the best of our knowledge, problem (**P**) has not been the subject of a rigorous numerical analysis yet, although some computational schemes have been devised in the literature. In Lachand-Robert and Oudet (2005) the authors propose an algorithm for minimizing functionals over sets of convex bodies. Similar to the setting in Buttazzo and Guasoni (1997), they consider only geometric functionals of the form

$$F(\Omega) = \int_{\partial\Omega} j(x, \nu(x), \varphi(x))\,\mathrm{d}\mathcal{H}^{d-1},$$

where $\varphi(x)$ is the signed distance of the supporting hyperplane of Ω at x to the origin 0. The proposed algorithm is based on approximating convex bodies by the intersection of finitely many half spaces. Since the topology of this intersection changes throughout the algorithm, it is not clear how this algorithm can be coupled with a (finite element) discretization of a PDE. In the recent preprint Antunes and Bogosel (2018), the authors approximate the support function of a convex body by its Fourier series decomposition ($d = 2$) and by its spherical harmonic decomposition ($d = 3$). The convexity amounts to an inequality constraint on the unit sphere $S^{d-1} \subset \mathbb{R}^d$. This convexity constraint is discretized by its sampling in a finite number of points.

Other related contributions address optimization problems over classes of convex functions. The developed methods are of interest for the treatment of problem (**P**) if admissible convex shapes can be represented via superlevel sets of convex functions over a fixed domain, i.e., if they are of the form $\Omega = \{(x', x_n) \in D \times [-M, 0] : \phi(x') \leq x_n \leq 0\}$ with a convex set $D \subset \mathbb{R}^{d-1}$ and a convex function $\phi : D \to [-M, 0]$ for some $M > 0$. For various approaches to solve optimization problems over sets of convex functions, we refer to Mirebeau (2016) and the references therein.

Our algorithm to approximate optimal convex shapes is based on a convergence result for finite element discretizations which identify admissible discrete shapes with polyhedral domains given by classes of triangulations. The iteration computes finite element diffeomorphisms to deform the domains via suitable constrained representatives of shape derivatives. The constraints realize a linearized convexity condition. A subsequent line search step determines an optimal step size. The inner product used to represent the shape derivative is chosen in a way that avoids mesh degeneracies. We present various numerical experiments that illustrate the features of the devised method and the peculiarities of the mathematical problem.

The outline of this article is as follows. Section 2 is devoted to a general existence result which serves as a template for the convergence of discretizations which are discussed in section 3. Our iterative algorithm is formulated in section 4. Its performance and qualitative features of optimal convex shapes are illustrated in section 5.

2. Existence of optimal convex shapes. For convenience, we repeat the PDE constrained shape optimization problem formulated in the introduction:

$$(\mathbf{P}) \qquad \begin{aligned} \text{Minimize} \quad & \int_\Omega j(x, u(x), \nabla u(x))\,\mathrm{d}x \\ \text{w.r.t.} \quad & \Omega \subset \mathbb{R}^d, u \in H^1_0(\Omega), \\ \text{s.t.} \quad & -\Delta u = f \text{ in } \Omega \text{ and } \Omega \subset Q \text{ convex and open.} \end{aligned}$$

Here, $Q \subset \mathbb{R}^d$ is bounded and convex, and $f \in L^2(Q)$. Conditions on $j : Q \times \mathbb{R} \times \mathbb{R}^d \to \mathbb{R}$ are formulated below. We remark that the empty set $\Omega = \emptyset$ is an admissible point of (**P**) with objective value 0. The following existence result is a consequence of the concept of γ-convergence of sets (see (Attouch et al., 2014, Def. 5.8.2)) and the compactness result for sequences of convex sets from Buttazzo and Guasoni (1997). The latter result states that for a sequence (Ω_n) of convex sets with $K \subset \Omega_n \subset Q$ for a compact set $K \subset \Omega$ (which is allowed to be empty), there exists a convex set Ω with $K \subset \Omega \subset Q$ such that the characteristic functions $\chi_{\Omega_{n_k}}$ of a subsequence (Ω_{n_k}) converge to χ_Ω in variation; i.e., the distributional gradients $\nabla\chi_{\Omega_{n_k}}$ converge to $\nabla\chi_\Omega$ as measures w.r.t. the weak-$\star$ topology, and the sequence of total variations converges. For the convenience of the reader, we include the short proof.

PROPOSITION 2.1 (existence). *Assume that j is a Carathéodory function (i.e., measurable in the first and continuous in its remaining arguments) and that there exist $a \in L^1(Q)$ and $c \geq 0$ such that*

$$|j(x, s, z)| \leq a(x) + c(|s|^p + |z|^2)$$

*with $p = 2d/(d-2)$ if $d > 2$ and $p < \infty$ if $d = 2$. Then there exists an optimal pair (Ω, u) for (**P**).*

Proof. (i) *Choice of an infimizing sequence.* First, we note that $\|\nabla\widetilde{u}\|_{L^2(Q)} \leq \|\nabla u\|_{L^2(\Omega)} \leq c_P\|f\|_{L^2(Q)}$ holds for every convex domain Ω and corresponding solution

$u \in H_0^1(\Omega)$ with trivial extension $\widetilde{u}$ to Q of the Poisson problem. Thus, we have that the objective function is bounded from below on the set of admissible pairs (Ω, u). Therefore, we can select an infimizing sequence (Ω_n, u_n).

(ii) *Existence of accumulation points.* Using Lemma 3.1 from Buttazzo and Guasoni (1997), we find that there exist an open convex set $\Omega \subset Q$ and a subsequence of $(\Omega_n)_n$ (which is not relabeled in what follows) such that the sequence of distributional derivatives of the characteristic functions χ_{Ω_n} converges in variation to χ_Ω. In particular, we have by the compact embedding of $BV(\Omega)$ into $L^1(\Omega)$ (see, e.g., Theorem 10.1.4 in Attouch et al. (2014)) that the characteristic functions χ_{Ω_n} converge strongly in $L^1(Q)$ to χ_Ω. Moreover, it follows from Lemma 4.2 in Buttazzo and Guasoni (1997) that for every $\varepsilon > 0$ there exists $N > 0$ such that for the symmetric set difference

$$\Omega_n \triangle \Omega = (\Omega \setminus \Omega_n) \cup (\Omega_n \setminus \Omega)$$

we have for all $n \geq N$ that

$$\Omega_n \triangle \Omega \subset \{x \in Q : \operatorname{dist}(x, \partial\Omega) \leq \varepsilon\}. \tag{2.1}$$

We trivially extend the solutions $u_n \in H_0^1(\Omega_n)$ to functions $\widetilde{u}_n \in H_0^1(Q)$. Since this defines a bounded sequence in $H_0^1(Q)$, we may extract a weakly convergent subsequence with limit $\widetilde{u} \in H_0^1(Q)$. We have to show that $\widetilde{u}|_\Omega$ solves the Poisson problem on Ω. For this let $\phi \in C^1(Q)$ be compactly supported in Ω. For $n \geq N$ with N sufficiently large we deduce from (2.1) that $\phi \in C_c^1(\Omega_n)$. Hence, it follows that

$$\int_\Omega \nabla u \cdot \nabla \phi \, \mathrm{d}x = \lim_{n\to\infty} \int_Q \nabla \widetilde{u}_n \cdot \nabla \phi \, \mathrm{d}x = \lim_{n\to\infty} \int_Q f\phi \, \mathrm{d}x = \int_\Omega f\phi \, \mathrm{d}x.$$

It remains to show that $u := \widetilde{u}|_\Omega$ belongs to $H_0^1(\Omega)$. To this end, let A be a compact subset in $Q \setminus \overline{\Omega}$. For $n \geq N$ with N sufficiently large we have $\widetilde{u}_n|_A = 0$, and hence

$$\|\widetilde{u}\|_{L^2(A)} = \|\widetilde{u} - \widetilde{u}_n\|_{L^2(A)} \leq \|\widetilde{u} - \widetilde{u}_n\|_{L^2(Q)} \to 0$$

as $n \to \infty$. Hence $\widetilde{u}|_A = 0$ for every compact subset $A \subset Q \setminus \overline{\Omega}$. We may therefore approximate u by a sequence of smooth functions that are compactly supported in Ω, and this implies $u|_{\partial\Omega} = 0$, i.e., $u \in H_0^1(\Omega)$.

(iii) *Optimality of the limit.* To show that the constructed pair (Ω, u) solves the optimization problem, we first note that the (sub)sequence $(\widetilde{u}_n)$ converges strongly to $\widetilde{u}$ in $H_0^1(Q)$. This is an immediate consequence of the identities

$$\int_Q |\nabla \widetilde{u}|^2 \, \mathrm{d}x = \int_Q fu \, \mathrm{d}x = \lim_{n\to\infty} \int_Q f\widetilde{u}_n \, \mathrm{d}x = \lim_{n\to\infty} \int_Q |\nabla \widetilde{u}_n|^2 \, \mathrm{d}x.$$

With the assumptions on j it follows from an application of Fatou's lemma that the objective functional is γ-continuous (see (Attouch et al., 2014, p. 213) for details), i.e., that

$$\int_{\Omega_n} j(x, u_n(x), \nabla u_n(x)) \, \mathrm{d}x \to \int_\Omega j(x, u(x), \nabla u(x)) \, \mathrm{d}x,$$

which implies that the pair (Ω, u) solves the shape optimization problem. ∎

We remark that for a simpler class of objective functionals, a related existence result can be found in (Delfour and Zolésio, 2001, Thm. 6.2 in Chapter 6). Generalizations of Proposition 2.1 can be made concerning boundary terms.

Remark 2.2 (boundary terms). Noting that the sequence of convex sets (Ω_n) converges in variation to Ω, we may incorporate a boundary term

$$\int_{\partial\Omega} g(x,\nu(x))d\mathcal{H}^{n-1} = \int_Q g(x,\nu)\mathrm{d}|D\chi_\Omega|$$

in the objective functional; cf. Buttazzo and Guasoni (1997).

The following example shows that shape optimization problems are often ill posed if the class of admissible domains is too large.

Example 2.3 (nonexistence without convexity assumption). To construct our counterexample, we use the classical construction from Cioranescu and Murat (1997). Let an arbitrary bounded and open set $Q \subset \mathbb{R}^d$ be given. We construct a perforated domain, as described in (Cioranescu and Murat, 1997, Ex. 2.1). That is, we choose a sequence $\{\varepsilon_n\}_{n\in\mathbb{N}} \subset (0,\infty)$ with $\varepsilon_n \to 0$ and set

$$r_n = \begin{cases} \exp^{-\varepsilon_n^{-2}} & \text{if } d = 2, \\ \varepsilon_n^{d/(d-2)} & \text{if } d > 2. \end{cases}$$

For each $\mathbf{i} \in \mathbb{Z}^d$, let $T_{\mathbf{i}}^n = B_{r_n}(\varepsilon_n\,\mathbf{i})$ be the closed ball with radius r_n centered at $\varepsilon_n\,\mathbf{i}$. Now, the perforated domain is given by

$$\Omega_n = Q \setminus \bigcup_{\mathbf{i}\in\mathbb{Z}^d} T_{\mathbf{i}}^n.$$

As $n \to \infty$, both the distance ε_n and the radius r_n of the holes go to 0. Now we define $u_n \in H_0^1(\Omega_n)$ as the weak solution of

$$-\Delta u_n = 1 \quad \text{in } \Omega_n, \qquad u_n = 0 \quad \text{on } \partial\Omega_n,$$

and extend u_n by 0 to a function in $H_0^1(Q)$. By (Cioranescu and Murat, 1997, Thms. 1.2, 2.2), u_n converges weakly in $H_0^1(Q)$ to the weak solution $\hat{u} \in H_0^1(Q)$ of

$$-\Delta\hat{u} + \mu\,\hat{u} = 1 \quad \text{in } Q, \qquad \hat{u} = 0 \quad \text{on } \partial Q,$$

for some $\mu > 0$. For the precise value of μ, we refer the reader to (Cioranescu and Murat, 1997, (2.3)). After this preparation, we choose the objective

$$j(x,u,g) := -1 + (u - \hat{u}(x))^2.$$

Let us check that for an arbitrary open set $\Omega \subset Q$ with associated state u, we have

$$\int_\Omega j(x,u(x),\nabla u(x))\,\mathrm{d}x > -\mathcal{L}^d(Q).$$

Here, $\mathcal{L}^d$ is the d-dimensional Lebesgue measure. Indeed, it is clear that $\mathcal{L}^d(\Omega) \le \mathcal{L}^d(Q)$. Moreover, one can check that $u \ne \hat{u}$ in $L^2(\Omega)$. This follows, e.g., from inner regularity and

$$-\Delta u(x) = 1 \ne 1 - \mu\,\hat{u}(x) = -\Delta\hat{u}(x)$$

for all inner points $x \in \Omega$. On the other hand, the sequence Ω_n together with the associated states u_n satisfies

$$\int_{\Omega_n} j(x,u_n(x),\nabla u_n(x))\,\mathrm{d}x = -\mathcal{L}^d(\Omega_n) + \int_{\Omega_n} (u_n - \hat{u})^2\,\mathrm{d}x \to -\mathcal{L}^d(Q),$$

since the Lebesgue measure of the holes tends to zero and $u_n \rightharpoonup \hat{u}$ in $H_0^1(Q)$ implies $u \to \hat{u}$ in $L^2(Q)$. Thus, the infimal value $-\mathcal{L}^d(Q)$ is not attained.

3. Convergence of discretizations. In this section we discuss convergence results for suitable discretizations of problem (**P**). The first one is a general statement under moderate assumptions, while the second one requires further conditions but serves as the basis for the iterative scheme devised in section 4 below.

3.1. Abstract convergence analysis. For a universal constant $c_{\text{usr}} > 0$ we consider the class $\mathbb{T}_{c_{\text{usr}}}$ of conforming, uniformly shape regular triangulations $\mathcal{T}_h$ of polyhedral subsets of $\mathbb{R}^d$ such that $h_T/\varrho_T \le c_{\text{usr}}$ for all elements $T \in \mathcal{T}_h$ with diameter $h_T \le h$ and inner radius ϱ_T. For a discretization fineness $h > 0$ we consider the following discrete version of (**P**):

$$(\mathbf{P}_h) \qquad \begin{aligned} &\text{Minimize} && \int_{\Omega_h} j(x, u_h(x), \nabla u_h(x))\,\mathrm{d}x \\ &\text{w.r.t.} && \Omega_h \subset \mathbb{R}^d,\ \mathcal{T}_h \in \mathbb{T}_{c_{\text{usr}}} \text{ triangulation of } \Omega_h,\ u_h \in \mathcal{S}_0^1(\mathcal{T}_h), \\ &\text{s.t.} && -\Delta_h u_h = f_h \text{ in } \Omega_h \text{ and } \Omega_h \subset Q \text{ convex and open.} \end{aligned}$$

Here, $\mathcal{S}_0^1(\mathcal{T}_h) \subset H_0^1(\Omega_h)$ consists of all piecewise affine, globally continuous functions in $H_0^1(\Omega_h)$. The identity $-\Delta_h u_h = f_h$ represents the discrete formulation of the Poisson problem; i.e., $u_h \in \mathcal{S}_0^1(\mathcal{T}_h)$ satisfies

$$\int_{\Omega_h} \nabla u_h \cdot \nabla v_h \,\mathrm{d}x = \int_{\Omega_h} f v_h \,\mathrm{d}x$$

for all $v_h \in \mathcal{S}_0^1(\mathcal{T}_h)$. Note that the formulation $(\mathbf{P}_h)$ may not admit a minimizer since triangulations corresponding to infimizing sequences may not have admissible accumulation points as the number of nodes in the corresponding triangulations might be unbounded. However, for the statements of the following results only the existence of almost-infimizing points is necessary. Further constraints such as a bound on the number of elements in $\mathcal{T}_h$, e.g., $\#\mathcal{T}_h \le ch^{-d}$, can be included to obtain a more practical minimization problem that admits a solution due to finite dimensionality. The following estimate provides an approximation result for certain regular solutions and will be used to justify the general convergence of the discretization below.

PROPOSITION 3.1 (consistency). *Assume that $d = 2$. Let an optimal pair (Ω, u) be such that Ω is convex with piecewise C^2 regular boundary and that the solution $u \in H_0^1(\Omega)$ of the corresponding Poisson problem in Ω satisfies $u \in H^2(\Omega) \cap W^{1,\infty}(\Omega)$, and assume that j is such that the functional J defined by*

$$J(A, v) = \int_A j(x, v(x), \nabla v(x))\,\mathrm{d}x$$

satisfies for some constant $c_J \ge 0$ the estimate

$$\big|J(A, v) - J(A, w)\big| \le c_J(1 + \|\nabla v\|_{L^2(A)} + \|\nabla w\|_{L^2(A)})\|\nabla(v - w)\|_{L^2(A)}$$

for every open set $A \subset Q$ and $v, w \in H_0^1(A)$. Then there exist admissible tuples $(\Omega_h, \mathcal{T}_h, u_h)$ for $(\mathbf{P}_h)$ and $(\Omega_h, \widehat{u}^{(h)})$ for $(\mathbf{P})$ such that $\Omega_h \subset \Omega$,

$$\Omega_h \triangle \Omega \subset \{x \in \Omega : \operatorname{dist}(x, \partial\Omega) \le ch^2\},$$

and

$$\|\nabla(u - \widetilde{u}_h)\|_{L^2(\Omega)} + \|\nabla(u_h - \widehat{u}^{(h)})\|_{L^2(\Omega_h)} \le ch.$$

In particular, we have

$$0 \le J(\Omega_h, \widehat{u}^{(h)}) - J(\Omega, u) \le ch.$$

Proof. We first choose an interpolating triangulation $\mathcal{T}_h$ of Ω with maximal mesh-size $h > 0$. In the two-dimensional situation under consideration, the interior of the union of elements in $\mathcal{T}_h$ defines a convex open set $\Omega_h \subset \Omega$. Standard results on boundary approximation (cf., e.g., Dziuk (2010) and (Bartels, 2016, Prop. 3.7)) yield that the corresponding finite element approximation of u satisfies the asserted estimate. The function

$$\widehat{u}^{(h)} = u_h + r^{(h)}$$

is defined with the correction $r^{(h)} \in H_0^1(\Omega_h)$ that satisfies

$$\int_{\Omega_h} \nabla r^{(h)} \cdot \nabla v \,\mathrm{d}x = \int_{\Omega_h} f v \,\mathrm{d}x - \int_{\Omega_h} \nabla u_h \cdot \nabla v \,\mathrm{d}x$$

for all $v \in H_0^1(\Omega_h)$ so that we have $-\Delta \widehat{u}^{(h)} = f$ in Ω_h. It follows that

$$\begin{aligned}
\|\nabla r^{(h)}\|_{L^2(\Omega_h)}^2 &= \int_{\Omega_h} f\, r^{(h)} \,\mathrm{d}x - \int_{\Omega_h} \nabla u_h \cdot \nabla r^{(h)} \,\mathrm{d}x \\
&= \int_{\Omega_h} \nabla u \cdot \nabla r^{(h)} \,\mathrm{d}x - \int_{\Omega_h} \nabla u_h \cdot \nabla r^{(h)} \,\mathrm{d}x \\
&\le \|\nabla (u - u_h)\|_{L^2(\Omega_h)} \|\nabla r^{(h)}\|_{L^2(\Omega_h)}.
\end{aligned}$$

The assumed local Lipschitz estimate for J and the fact that $J(\Omega, u) \le J(\Omega_h, \widehat{u}^{(h)})$ imply the result. ∎

Remark 3.2. Note that an interpolating polygonal domain of a convex domain is in general not convex if $d = 3$ so that the arguments of the proof cannot be directly generalized to that setting.

The second result concerns the stability of the method, i.e., that solutions for $(\mathbf{P}_h)$ accumulate at solutions for $(\mathbf{P})$ as the mesh size tends to zero.

PROPOSITION 3.3 (stability). *Let $d = 2$, assume that j satisfies the conditions of Proposition* 2.1 *and Proposition* 3.1, *and let $(\Omega_h, \mathcal{T}_h, u_h)_{h>0}$ be a sequence of discrete solutions for $(\mathbf{P}_h)$. Then, every accumulation pair (Ω, u) solves $(\mathbf{P})$.*

Proof. We argue as in the proof of Proposition 2.1. Accumulation points Ω of the sequence of convex sets (Ω_h) are convex and the finite element solutions are bounded in $H_0^1(Q)$ with weak accumulation points $u \in H_0^1(\Omega)$. To show that every such point solves the Poisson problem in Ω we choose a smooth, compactly supported function $\phi \in C_c^\infty(\Omega)$ and note that by the uniform convergence $\Omega_h \triangle \Omega \to 0$ stated in (2.1) we have for h sufficiently small that the nodal interpolant $\phi_h = \mathcal{I}_h \phi \in \mathcal{S}^1(\mathcal{T}_h)$ satisfies $\phi_h \in H_0^1(\Omega_h)$. Moreover, we deduce from nodal interpolation results and the uniform control on the shape of the elements that (after trivial extension to Q) we have $\phi_h \to \phi$ in $H^1(Q)$. These properties lead to the relation

$$\int_Q \nabla u \cdot \nabla \phi \,\mathrm{d}x = \lim_{h\to 0} \int_Q \nabla u_h \cdot \nabla \phi_h \,\mathrm{d}x = \lim_{h \to 0} \int_Q f \phi_h \,\mathrm{d}x = \int_Q f \phi \,\mathrm{d}x.$$

Arguing as in the proof of Proposition 2.1 it follows that the finite element solutions converge strongly in $H_0^1(Q)$. With the results from (Attouch et al., 2014, p. 213) the conditions on j yield that

$$J(\Omega, u) \le \liminf_{h \to 0} J(\Omega_h, u_h).$$

It remains to show that the pair (Ω, u) is optimal. For this, we note that for an optimal pair (Ω^*, u^*) the convex set Ω^* can be approximated by smooth convex domains contained in Ω^*, and also if the right-hand side f is regularized, then the corresponding smooth solutions of the Poisson problems converge strongly in H^1 to u^*; see (Dobrowolski, 2006, p. 141) for related details. Hence, Proposition 3.1 implies that the limit of the sequence $J(\Omega_h, u_h)$ is bounded from above by the optimal continuous value. Since (Ω, u) is admissible, we deduce that it solves $(\mathbf{P})$. ∎

3.2. Deformed triangulations. The discrete formulation $(\mathbf{P}_h)$ is of limited practical interest. Under a regularity assumption on a solution of the continuous formulation $(\mathbf{P})$ we devise a convergent discrete scheme that admits a solution. The admissible discrete domains are obtained from certain discrete deformations of a given convex reference domain $\widehat{\Omega}$:

$$(\mathbf{P}'_h)\qquad \begin{aligned} &\text{Minimize} && \int_{\Omega_h} j(x, u_h(x), \nabla u_h(x))\,\mathrm{d}x \\ &\text{w.r.t.} && \Phi_h \in \mathcal{S}^1(\widehat{\mathcal{T}}_h)^d,\ \mathcal{T}_h \text{ triangulation of } \Omega_h,\ u_h \in \mathcal{S}^1_0(\mathcal{T}_h), \\ &\text{s.t.} && \|D\Phi_h\|_{L^\infty(\widehat{\Omega})} + \|[D\Phi_h]^{-1}\|_{L^\infty(\widehat{\Omega})} \le c_0, \\ &&& \Omega_h = \Phi_h(\widehat{\Omega}) \subset Q \text{ convex and open},\ \mathcal{T}_h = \Phi_h(\widehat{\mathcal{T}}_h) \\ &&& -\Delta_h u_h = f_h \text{ in } \Omega_h,\ u_h = 0 \text{ on } \partial\Omega_h. \end{aligned}$$

Here, $\widehat{\mathcal{T}}_h$ is a fixed regular triangulation of the convex reference domain $\widehat{\Omega}$. The notation $\Phi_h(\widehat{\mathcal{T}}_h)$ represents the triangulation $\mathcal{T}_h$ of Ω_h that is obtained by applying Φ_h to the elements in $\widehat{\mathcal{T}}_h$. Note that Φ_h maps triangles of $\widehat{\mathcal{T}}_h$ to triangles, since it is affine on each triangle of $\widehat{\mathcal{T}}_h$.

PROPOSITION 3.4. *Assume that (Ω, u) is a solution for $(\mathbf{P})$ such that $\Omega = \Phi(\widehat{\Omega})$ with an injective deformation $\Phi \in W^{1,\infty}(\widehat{\Omega}; \mathbb{R}^d)$, satisfying*

$$\|D\Phi\|_{L^\infty(\widehat{\Omega})} + \|[D\Phi]^{-1}\|_{L^\infty(\widehat{\Omega})} \le c_0'$$

and $\Phi|_T \in W^{2,\infty}(T; \mathbb{R}^d)$ with $\|D^2\Phi\|_{L^\infty(T)} \le c_0''$ for all $T \in \widehat{\mathcal{T}}_h$. For h sufficiently small and c_0 sufficiently large we have the following results:

(i) *There exists a discrete solution (Ω_h, u_h) for $(\mathbf{P}'_h)$.*

(ii) *If $d = 2$, there exists an admissible pair (Ω_h, u_h) obeying the bounds of Proposition 3.1 provided that the optimal pair (Ω, u) satisfies the assumptions of Proposition 3.1.*

(iii) *If $d = 2$ and $(\Omega_h, u_h)_{h>0}$ is a sequence of discrete solutions, then every accumulation point for $h \to 0$ solves the continuous formulation.*

Proof. (i) The existence of a solution (Φ_h, Ω_h, u_h) follows from continuity properties of the objective function and the boundedness of admissible elements.

(ii) We define $\Phi_h = \widehat{\mathcal{I}}_h \Phi$ as the nodal interpolant of Φ on $\widehat{\Omega}$. As $\|D\Phi_h - D\Phi\|_{L^\infty(T)} \le ch\|D^2\Phi\|_{L^\infty(T)}$ for all $T \in \widehat{\mathcal{T}}_h$ we find that Φ_h is admissible in $(\mathbf{P}'_h)$. Then, $\Omega_h = \Phi_h(\widehat{\Omega})$ is a polygonal domain whose boundary interpolates the boundary of Ω so that it is convex (in the considered two-dimensional situation). The finite element solution u_h on Ω_h then approximates the exact solution $u \in H^1_0(\Omega) \cap H^2(\Omega)$ of the Poisson problem on the convex domain Ω.

(iii) For a sequence of discrete solutions it follows as in Proposition 3.3 that accumulation points (Ω, u) are admissible in $(\mathbf{P})$. By the approximation result (ii) it follows that these are optimal. ∎

Remark 3.5. As above, an interpolating polygonal domain of a convex domain is in general not convex if $d = 3$ so that the proposition cannot be directly generalized to that setting.

The elementwise regularity assumption on a solution Φ cannot be avoided in general.

Example 3.6 (noninvertibility of the interpolant). Let $\Phi : B_{1,\pi/2}(0) \to B_{1,\pi}(0)$ be the mapping that maps the quarter-disk with radius 1 to the half-disk with radius 1 by doubling the angle of every point in its polar coordinates, i.e., $\Phi(r, \phi) = (r, 2\phi)$ for $0 < r < 1$ and $0 < \phi < \pi/2$. Then Φ and Φ^{-1} are Lipschitz continuous. For every $0 < h \le 1$ the vertices of the triangle $T = \operatorname{conv}\{(0, 0), (h, 0), (0, h)\}$ are mapped onto the line segment $[-h, h] \times \{0\}$. Hence, the interpolant $\Phi_h = \mathcal{I}_h\Phi$ cannot be a diffeomorphism on T.

4. Numerical realization. In this section, we describe a possibility to solve a slight variation concerning the treatment of the bounds on the diffeomorphism Φ_h (see subsection 4.3 for details) of the discretization ($\mathbf{P}'_h$) of ($\mathbf{P}$). For this, let Ω_h be a convex polygon together with a regular triangulation $\mathcal{T}_h$. We introduce the discrete shape functional J_h via

$$J_h(\Omega_h) := \int_{\Omega_h} j(x, u_h(x), \nabla u_h(x)) \,\mathrm{d}x, \tag{4.1}$$

where $u_h \in \mathcal{S}^1_0(\mathcal{T}_h)$ is the solution of the discretized state equation

$$\int_{\Omega_h} \nabla u_h \cdot \nabla v_h \,\mathrm{d}x = \int_{\Omega_h} f\, v_h \,\mathrm{d}x \qquad \forall v_h \in \mathcal{S}^1_0(\mathcal{T}_h).$$

In fact, J_h depends not only on Ω_h but also on the underlying triangulation $\mathcal{T}_h$. However, this dependence is not explicitly mentioned for ease of the presentation.

We are going to optimize this domain by moving the vertices in the triangulation $\mathcal{T}_h$. We will see that this is consistent with a discrete version of the perturbation of identity. Indeed, if $V_h \in \mathcal{S}^1(\mathcal{T}_h)^d$ is a piecewise linear deformation field, then $T_t := I + t\, V_h$ describes a piecewise linear perturbation leading to the deformed triangulation $T_t(\mathcal{T}_h)$, in which the position of each vertex x_j is changed to $x_j + t\, V_h(x_j)$. Note that $V_h(x_j)$ are precisely the degrees of freedom of the finite element function V_h. Moreover, this deformation has the important property

$$v_h \circ T_t^{-1} \in \mathcal{S}^1_0(T_t(\mathcal{T}_h)) \quad \Longleftrightarrow \quad v_h \in \mathcal{S}^1_0(\mathcal{T}_h)$$

for all functions $v_h : \Omega \to \mathbb{R}$.

Due to this property, it is possible to derive a shape derivative for the discrete functional J_h by standard procedures; cf., e.g., (Delfour and Zolésio, 2011, Chapter 10). This leads to the expression

$$\begin{aligned} J_h'(\Omega_h; V_h) = \int_{\Omega_h} & j_x(\cdot) \cdot V_h - j_v(\cdot) \cdot DV_h^\top \nabla u_h + \nabla p_h^\top \big[-DV_h - DV_h^\top + \operatorname{div}(V_h)\, I\big] \nabla u_h \\ & - \operatorname{div}(f\, V_h)\, p_h + j(\cdot)\, \operatorname{div}(V_h) \,\mathrm{d}x \end{aligned} \tag{4.2}$$

for all $V_h \in \mathcal{S}^1(\mathcal{T}_h)^d$. Here, $(\cdot)$ abbreviates the argument $(x, u_h(x), \nabla u_h(x))$. Moreover, $p_h \in \mathcal{S}^1_0(\mathcal{T}_h)$ is the discrete adjoint state which solves the adjoint equation

$$\int_{\Omega_h} \nabla p_h \cdot \nabla w_h \,\mathrm{d}x = \int_{\Omega_h} j_u(\cdot)\, w_h + j_v(\cdot) \cdot \nabla w_h \,\mathrm{d}x \qquad \forall w_h \in \mathcal{S}^1_0(\mathcal{T}_h). \tag{4.3}$$

In order to formulate an implementable algorithm, we have to compute a "good" representing deformation field V_h from the shape derivative $J_h'(\Omega_h; \cdot)$. Consequently, this deformation field is used to update the domain Ω_h via $(I + t\, V_h)(\Omega_h)$, where t is a suitable step size. For the calculation of V_h, three important points are to be considered, and these will be described in the next three sections:

(i) The shape derivative $J_h'(\Omega_h; \cdot)$ is an element of the dual space of $\mathcal{S}^1(\mathcal{T}_h)^d$ and has to be represented by an element of $\mathcal{S}^1(\mathcal{T}_h)^d$ in an appropriate inner product. This will be considered in subsection 4.1.

(ii) At some point in our algorithm, we have to respect the convexity constraint which is posed in the problem under consideration. We will use deformation fields which are (in a certain sense) first-order feasible; see subsection 4.2.

(iii) The Hadamard form of the shape derivative shows that (in certain situations) the directional derivative $J'(\Omega; V)$ only depends on the normal trace of V. This is no longer the case for $J_h'(\Omega_h; V_h)$, since the functional $J_h(\Omega_h)$ also depends on the location of the inner nodes of the triangulation $\mathcal{T}_h$. This problem and a possible solution are addressed in subsection 4.3.

With these preparations, we comment on a possible line-search strategy (subsection 4.4) and state an implementable algorithm (subsection 4.5).

From now on, we drop the constraint $\Omega \subset Q$. On the one hand, for the examples considered in section 5, the objective ensures that the iterates Ω_h remain in a compact subset of $\mathbb{R}^d$. On the other hand, such a constraint can be implemented similarly to the convexity constraint (see subsection 4.2): One just needs to ensure that the boundary nodes of Ω_h remain in Q, and often (depending on Q), this can be reformulated via differentiable, nonlinear inequality constraints.

4.1. Computation of a shape gradient. There are many possibilities for computing a deformation field V_h from the linear functional $J_h'(\Omega_h; \cdot)$. We follow the approach proposed in (Schulz et al., 2016, section 3). To this end, we introduce the elasticity bilinear form

$$\mathcal{E}_h(V_h, W_h) := \int_{\Omega_h} 2\,\mu\,\boldsymbol{\varepsilon}(V_h) : \boldsymbol{\varepsilon}(W_h) + \lambda \operatorname{trace}(\boldsymbol{\varepsilon}(V_h)) \operatorname{trace}(\boldsymbol{\varepsilon}(W_h)) + \delta\, V_h \cdot W_h \,\mathrm{d}x$$

for $V_h, W_h \in \mathcal{S}^1(\mathcal{T}_h)^d$. Here, $\boldsymbol{\varepsilon}(V_h) := (DV_h + DV_h^\top)/2$ is the linearized strain tensor. Moreover, $\mu, \lambda > 0$ are the Lamé parameters and $\delta > 0$ is a damping parameter such that $\mathcal{E}_h$ becomes coercive on $\mathcal{S}^1(\mathcal{T}_h)^d$.

Now, one possibility to compute a deformation field V_h is to solve

$$\mathcal{E}_h(V_h, W_h) = -J_h'(\Omega_h; W_h) \qquad \forall W_h \in \mathcal{S}^1(\mathcal{T}_h)^d. \tag{4.4}$$

Note that this is equivalent to solving the following minimization problem:

$$\begin{aligned} \text{Minimize} \quad & \frac{1}{2}\mathcal{E}_h(V_h, V_h) + J_h'(\Omega_h; V_h) \\ \text{w.r.t.} \quad & V_h \in \mathcal{S}^1(\mathcal{T}_h)^d. \end{aligned} \tag{4.5}$$

4.2. Feasible deformation fields. Using the deformation field V_h from (4.4) for deforming the domain Ω_h could lead to nonconvex domains. We incorporate the convexity constraint in such a way that the deformation field respects the convexity constraint to first order. We focus on the case of dimension $d = 2$ and briefly outline the case $d = 3$.

Let $\Omega_h \subset \mathbb{R}^2$ be a simply connected polygon, and let N be the number of boundary vertices of Ω_h with coordinates $x^{(j)} \in \mathbb{R}^2$, $j = 1, \ldots, N$, in counterclockwise order. It is easily seen that Ω_h is convex if and only if all the interior angles are less than or equal to π. By using the cross product, this, in turn, is equivalent to

$$C_j(X) := \left(x_1^{(j-1)} - x_1^{(j)}\right)\left(x_2^{(j+1)} - x_2^{(j)}\right) - \left(x_2^{(j-1)} - x_2^{(j)}\right)\left(x_1^{(j+1)} - x_1^{(j)}\right) \le 0 \tag{4.6}$$

for $j = 1, \ldots, N$, where we used the conventions $x^{(0)} = x^{(N)}$ and $x^{(N+1)} = x^{(1)}$. Moreover, the argument X represents the vector $(x^{(1)}, \ldots, x^{(N)})$. Likewise, the coordinates of the vertices of the perturbed domain are given by $x_j + t_i^0 V_h(x_j)$, where t_i^0 is an initial step size in iteration i. In a subsequent Armijo-like line search, the value t_i^0 is the largest possible step size; see subsection 4.4 below. Using these functions C_j, the convexity of the deformed domain $(I + t_i^0 V_h)(\Omega_h)$ is equivalent to $C_j(X + t_i^0 V_h(X)) \le 0$ for all $j = 1, \ldots, N$. We are going to use a first-order expansion of this quadratic constraint and obtain

$$C_j(X + t_i^0 V_h(X)) \approx C_j(X) + t_i^0\, DC_j(X)\, V_h(X) \overset{!}{\le} 0 \quad \forall j = 1, \ldots, N.$$

Therefore, we replace (4.5) by the constrained problem

$$\begin{aligned} \text{Minimize} \quad & \frac{1}{2}\mathcal{E}_h(V_h, V_h) + J_h'(\Omega_h; V_h) \\ \text{w.r.t.} \quad & V_h \in \mathcal{S}^1(\mathcal{T}_h)^d, \\ \text{s.t.} \quad & C_j(X) + t_i^0\, DC_j(X)\, V_h(X) \le 0 \quad \forall j = 1, \ldots, N. \end{aligned} \tag{4.7}$$

We remark that this is a convex quadratic program (QP).

We remark that the solution V_h of (4.7) may not be a descent direction for the objective; i.e., it might happen that $J_h'(\Omega_h; V_h) \ge 0$. Hence, we will use a merit function within the line search, and this will be discussed in subsection 4.4 below.

We briefly comment on the three-dimensional situation. Similar to the two-dimensional situation, we consider a 2-connected polyhedron Ω_h. Now, one can check that Ω_h is convex if each outer edge of Ω_h is convex in the sense that the dihedral angle between the two adjacent faces is less than or equal to π. We show that this can be written as a system of polynomial inequalities which is cubic w.r.t. the coordinates of the vertices of $\mathcal{T}_h$. To this end, we take an arbitrary outer edge with vertices $x^{(i)}$ and $x^{(j)}$. Relative to the vector from $x^{(i)}$ to $x^{(j)}$ we denote the third vertex of the left and right triangles by $x^{(l)}$ and $x^{(r)}$, respectively. The convexity of the edge can be characterized by the nonnegativity of the signed volume of the parallelepiped spanned by the vectors $x^{(l)} - x^{(i)}$, $x^{(l)} - x^{(i)}$, $x^{(r)} - x^{(i)}$, i.e.,

$$\left(x^{(l)} - x^{(i)}\right) \cdot \left(\left(x^{(j)} - x^{(i)}\right) \times \left(x^{(r)} - x^{(i)}\right)\right) \ge 0.$$

Now, a QP similar to (4.7) can be constructed analogously to the two-dimensional case.

4.3. Avoiding spurious interior deformations. We have already mentioned that the value of $J_h(\Omega_h)$ also depends on the positions of the interior nodes of the triangulation $\mathcal{T}_h$, since the discrete state u_h depends on all the nodes of $\mathcal{T}_h$. Therefore, using V_h governed by (4.5) or (4.7) would result also in an optimization of the nodes of the triangulation. In a more extreme case, we could even fix all the boundary nodes of the triangulation $\mathcal{T}_h$ in order to optimize the location of the interior nodes (this would result in zero Dirichlet boundary conditions for V_h in (4.5) or (4.7)). This may lead to degenerate triangulations.

In the discrete problem ($\mathbf{P}'_h$), this degeneracy of the triangulations was avoided by the bounds on $D\phi_h$ and $[D\phi_h]^{-1}$. In the numerical implementation, the realization of these constraints is rather cumbersome, and it is also not clear how the constant c_0 should be chosen. Therefore, we use a possible solution which is proposed in the recent paper Etling et al. (2020). Therein, the authors suggest restricting the set of admissible deformation fields in (4.5). Motivated by the continuous situation in which $J'(\Omega; V)$ only acts on the normal trace of V (due to Hadamard's structure theorem), it is reasonable to only consider those deformation fields V_h which result from a normal force. To this end, we introduce the operator $N_h : \mathcal{S}^1(\partial\mathcal{T}_h) \to (\mathcal{S}^1(\mathcal{T}_h)^d)^\star$ by requiring that for all $F_h \in \mathcal{S}^1(\partial\mathcal{T}_h)$ and $V_h \in \mathcal{S}^1(\mathcal{T}_h)^d$ we have

$$\langle N_h\, F_h, V_h\rangle := \int_{\partial\Omega_h} F_h\,(V_h \cdot n)\,\mathrm{d}s,$$

where $\mathcal{S}^1(\partial\mathcal{T}_h)$ are the piecewise linear and continuous functions on the boundary $\partial\Omega_h$. Now, a deformation field V_h results from a normal force $F_h \in \mathcal{S}^1(\partial\mathcal{T}_h)$ if

$$\mathcal{E}_h(V_h, W_h) = \langle N_h\, F_h, W_h\rangle \qquad \forall W_h \in \mathcal{S}^1(\mathcal{T}_h)^d.$$

Following this approach, we replace (4.7) by the following minimization problem:

$$\begin{aligned} \text{Minimize} \quad & \frac{1}{2}\mathcal{E}_h(V_h, V_h) + J'_h(\Omega_h; V_h) \\ \text{w.r.t} \quad & V_h \in \mathcal{S}^1(\mathcal{T}_h)^d, F_h \in \mathcal{S}^1(\partial\mathcal{T}_h), \\ \text{s.t.} \quad & C_j(X) + t_i^0\, DC_j(X)\, V_h \le 0 \quad \forall j = 1, \dots, N, \\ & \mathcal{E}_h(V_h, W_h) = \langle N_h\, F_h, W_h\rangle \quad \forall W_h \in \mathcal{S}^1(\mathcal{T}_h)^d. \end{aligned} \tag{4.8}$$

Again, problem (4.8) is a convex QP. The problem is feasible if, e.g., the current domain Ω_h is convex. Otherwise, Ω_h can be replaced by its convex hull.

4.4. Armijo-like line search with merit function. As explained above, we use the solution V_h of the convex QP (4.8) as a search direction using the perturbation of identity approach. That is, the next iterate is given by $\Omega_{h,t} := (I + t\, V_h)(\Omega_h)$, where $t > 0$ is a suitable step size. Since we consider a constrained problem, we use a merit function for the determination of suitable step sizes. To this end, we consider the merit function

$$\varphi(t) := J_h(\Omega_{h,t}) + M \sum_{j=1}^{N} \big[C_j(X + t\, V_h(X))\big]^+$$

for some suitable parameter $M > 0$. It is easy to check that the (directional) derivative $\varphi'(0) = \lim_{t\searrow 0}(\varphi(t) - \varphi(0))/t$ is given by

$$\varphi'(0) = J'_h(\Omega_h; V_h) + M \sum_{j: C_j(X)=0} \big[DC_j(X)\, V_h(X)\big]^+ + M \sum_{j: C_j(X)>0} DC_j(X)\, V_h(X).$$

Moreover, if V_h is a feasible point of (4.8), the middle term vanishes due to the constraint in (4.8). Thus,

$$\varphi'(0) = J'_h(\Omega_h; V_h) + M \sum_{j: C_j(X)>0} DC_j(X)\, V_h(X). \tag{4.9}$$

Next, we obtain the result that the solution of (4.8) is a descent direction for the merit function φ if M is chosen large enough. Such a result is well known for the usage of merit functions in other optimization methods, e.g., within the sequential QP (SQP) method. The following statement follows from standard arguments.

LEMMA 4.1. *Let $V_h \neq 0$ be the solution of* (4.8). *Then,* $\varphi'(0) < 0$ *if* $M \geq t_0 \sup_{j=1,\dots,N} \lambda_j$, *where $\lambda \in \mathbb{R}^N$ is a Lagrange multiplier for V_h associated with the linearized convexity constraint in* (4.8).

Note that all the constraints in (4.8) are linear. Therefore, the existence of Lagrange multipliers at the solution V_h follows from standard arguments in optimization.

The overall line search with backtracking is performed as follows. We choose two parameters, $\sigma \in (0,1)$ and $\beta \in (0,1)$. Then, we select the smallest nonnegative integer k such that the Armijo condition

$$\varphi(t_i^0\,\beta^k) \leq \varphi(0) + \sigma\, t_i^0\, \beta^k\, \varphi'(0) \tag{4.10}$$

holds. Moreover, we need to check that the mesh quality is not affected too badly by the deformation V_h. Therefore, we check that

$$\frac{1}{2} \leq \det(I + t_i^0\,\beta^k\, DV_h) \leq 2, \qquad \|t_i^0\,\beta^k\, DV_h\| \leq 0.3 \tag{4.11}$$

are satisfied in the entire domain. Note that this amounts to checking three inequalities per cell of the mesh.

4.5. An implementable algorithm. Now, we are in the position to state an implementable algorithm; see Algorithm 1.

Algorithm 1: Solving a discretized problem.

Data: Initial domain Ω_h with triangulation $\mathcal{T}_h$
Initial step size $t_0 > 0$, convergence tolerance $\varepsilon_{\mathrm{tol}} > 0$,
Parameters $\beta \in (0,1)$, $\beta_M > 1$, $\sigma \in (0,1)$, $M > 0$
Result: Improved domain Ω_h
for $i \leftarrow 1$ **to** ∞ **do**
  Set initial step size for iteration i: $t_i^0 \leftarrow t_{i-1}/\beta$;
  Set up and solve the convex QP (4.8);
  if $\sqrt{|J_h'(\Omega_h; V_h)|} \leq \varepsilon_{\mathrm{tol}}$ **then**
    STOP, the current iterate Ω_h is almost stationary;
  end
  while $\varphi'(0) \geq 0$, *cf.* (4.9) **do**
    Increase the parameter M of the merit function: $M \leftarrow M\,\beta_M$;
  end
  $k \leftarrow 0$;
  while (4.10) *or* (4.11) *is violated* **do**
    $k \leftarrow k+1$;
  end
  $t_i \leftarrow t_i^0\,\beta^k$;
  Move the domain and triangulation according to $\Omega_h \leftarrow (I + t_i\,V_h)(\Omega_h)$, $\mathcal{T}_h \leftarrow (I + t_i\,V_h)(\mathcal{T}_h)$;
end

5. Numerical examples. In this section, we present numerical examples that illustrate the performance of the proposed algorithm and typical qualitative features of optimal convex shapes. We have implemented Algorithm 1 in Python. The implementation is available at Bartels and Wachsmuth (2018). For the finite-element discretization, we utilized the FEniCS framework (Alnæs et al. (2015); Logg et al. (2012)). The QP (4.8) was solved using the Operator Splitting Quadratic Program (OSQP) (Stellato et al. (2020)).

Before we discuss the different examples, we specify some of the required parameters:

$$\beta = \frac{1}{2}, \qquad \sigma = \frac{1}{10}, \qquad t_0 = 1, \qquad \beta_M = 10, \qquad M = 10^{-9}, \qquad \varepsilon_{\text{tol}} = 10^{-6}.$$

We remark that the precise value of the parameters t_0 and M is not of much importance, since both parameters get adapted during the iteration. The step sizes are increased and decreased automatically in steps 2 and 14, whereas M is increased in step 8 if V_h fails to be a descent direction of the merit function; see also Lemma 4.1.

For the elasticity operator $\mathcal{E}_h$, we have used the parameters

$$E = 1.0, \qquad \nu = 0.4, \qquad \lambda = \frac{\nu\, E}{(1+\nu)\,(1-2\,\nu)}, \qquad \mu = \frac{E}{2\,(1+\nu)}, \qquad \delta = 10.$$

5.1. Example in two dimensions. The first example shows that mesh deformations have to be carefully constructed to avoid degenerate triangulations. We consider problem (**P**) in two dimensions ($d = 2$); the objective is given by

$$\int_\Omega u \,\mathrm{d}x, \quad \text{i.e.,} \quad j(x, u, g) = u,$$

and the right-hand side in the PDE is

$$f(x_1, x_2) = 20\,(x_1 + 0.4 - x_2^2)^2 + x_1^2 + x_2^2 - 1.$$

The motivation for using this right-hand side f is as follows. Since we are going to minimize $\int_\Omega u\,\mathrm{d}x$, all points x with $f(x) \le 0$ are favorable since they decrease u (due to the maximum principle). Moreover, in the absence of a convexity constraint the optimal domain would be a subset of the nonconvex level $Z_0 = \{x \in \mathbb{R}^2 \mid f(x) \le 0\}$. Therefore, the shape optimization problem has to find a compromise between convexity of Ω and covering all of Z_0. The contour plot shown in Figure 5.1 indicates which regions are preferred by the optimization process. The numerical solution of the unconstrained shape optimization problem shown in the same figure is nonconvex, and its boundary is comparable to a contour line.

We chose the unit circle as the initial domain and started with a rather coarse discretization; see the upper left plot in Figure 5.2. We used Algorithm 1 to optimize this discrete domain. Afterwards, we applied a mesh refinement. This process was repeated to obtain optimal domains for five different refinements; see Algorithm 1. The overall runtime was roughly half an hour. The solution of the QPs (4.8) dominate the overall runtime. On the last three levels of discretization, one solution of the QP (4.8) was taking 0.05s, 0.5s, and 15s, respectively. The numbers of iterations (i.e., numbers of solutions of (4.8)) on the five refinement levels are 36, 36, 83, 95, and 130, respectively.

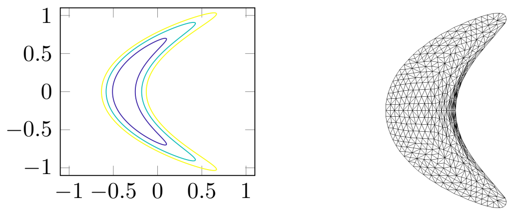

Fig. 5.1. *Contour plot of the forcing function f and optimal shape in the absence of a convexity constraint for the setting described in subsection* 5.1.

Fig. 5.2. *Scaled initial domain and coarse triangulation (left plot) and plots of optimal shapes for refined triangulations for the example discussed in subsection* 5.1. *The shapes of triangles near the origin tend to deteriorate.*

5.2. Example in two dimensions with nonsmooth minimizer. Our second example reveals that optimal convex shapes may have kinks and that the C^1 regularity result of Bucur (2003) does not apply in the considered framework. In this problem, we use the same data as in subsection 5.1, but

$$f(x_1, x_2) = -\frac{1}{2} + \frac{4}{5}\,(x_1^2 + x_2^2) + 2 \sum_{i=0}^{n-1} \exp\bigl(-8\,((x_1 - y_{1,i})^2 + (x_2 - y_{2,i})^2)\bigr) - \sum_{i=0}^{n-1} \exp\bigl(-8\,((x_1 - z_{1,i})^2 + (x_2 - z_{2,i})^2)\bigr)$$

with $n = 5$ and

$$y_{1,i} = \sin((i + 1/2)\,2\,\pi/n), \qquad z_{1,i} = \frac{6}{5}\,\sin(i\,2\,\pi/n),$$
$$y_{2,i} = \cos((i + 1/2)\,2\,\pi/n), \qquad z_{2,i} = \frac{6}{5}\,\cos(i\,2\,\pi/n).$$

This function f is designed to a have a fivefold rotational symmetry. In particular, the contribution of the second summation operator attracts the optimal shape towards the points $(z_{1,i}, z_{2,i})$, whereas the first summation operator repels the optimal shape from the points $(y_{1,i}, y_{2,i})$. As above, the contour plot of the function f indicates expected optimal shapes and is shown in Figure 5.3. A numerical solution of the unconstrained shape optimization problem shown in the same figure is nonconvex and has a smooth boundary. To solve the discrete problem with the convexity constraint, we performed the same steps as for the previous example. The initial mesh and the optimal mesh of five subsequent refinements can be seen in Figure 5.4. The overall runtime was 4 minutes and the solution times of the QP (4.8) are similar to previous example. The numbers of iterations per refinement level are 19, 20, 18, 15, and 14, respectively.

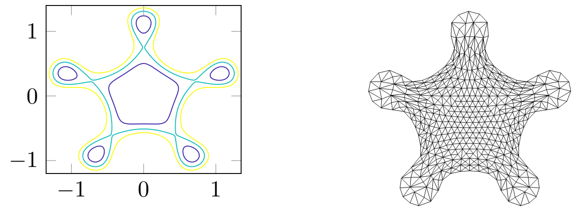

FIG. 5.3. *Contour plot of the forcing function f and optimal shape in the absence of a convexity constraint for the setting described in subsection* 5.2.

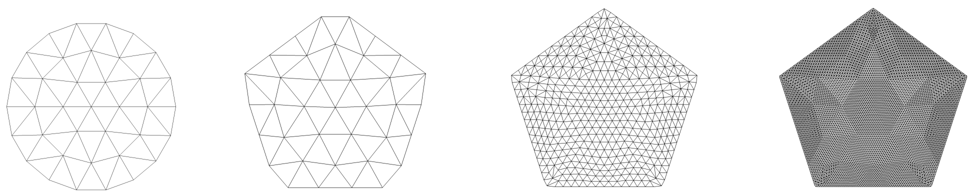

FIG. 5.4. *Scaled initial domain and coarse triangulation (left plot) and plots of optimal shapes for refined triangulations for the example discussed in subsection* 5.2. *Clearly defined kinks occur on the boundaries.*

5.3. Nonconvergence in three dimensions. As addressed briefly at the end of subsection 4.2, it is possible to apply Algorithm 1 also to three-dimensional shape optimization problems with convexity constraint. Our third example shows however that a direct discretization of the constraint can lead to nonconvergence. Instead of Dirichlet boundary conditions we impose Neumann boundary conditions and include a lower order term in the state equation; i.e., the modified shape optimization problem reads as follows:

$$\begin{aligned}
\text{Minimize} \quad & \int_\Omega u(x)\,\mathrm{d}x \\
\text{w.r.t.} \quad & \Omega \subset \mathbb{R}^3, u \in H^1(\Omega), \\
\text{s.t.} \quad & -\Delta u + u = f \text{ in } \Omega, \quad \frac{\partial u}{\partial n} = 0 \text{ on } \partial\Omega, \\
& \Omega \text{ convex and open.}
\end{aligned}$$

We chose $f(x) = x_1^2 + x_2^2 + x_3^2 - 1$. Since the problem is rotationally symmetric, we expect that the minimizer is a ball, which is obviously convex. We start with a tetrahedral grid on the cube $[-1/2, 1/2]^3$ (see the top left plot of Figure 5.5) and solved the discretized problem on three different mesh levels. The computational time was around 2 hours and the solution of the QP (4.8) took several minutes on the last mesh. The numbers of iterations were 16, 14, 23, respectively. The solutions are presented in Figure 5.5. As can be seen in this figure, the solutions are not rotationally symmetric and contain many flat parts on their boundary.

If we solve the same problem, but without the convexity constraint, we arrive at the bodies presented in Figure 5.6. In these plots, one can see that the optimal solution of the above problem might be indeed a ball. However, a closer inspection of Figure 5.6 reveals that the approximations are not convex; there are some “nonconvex

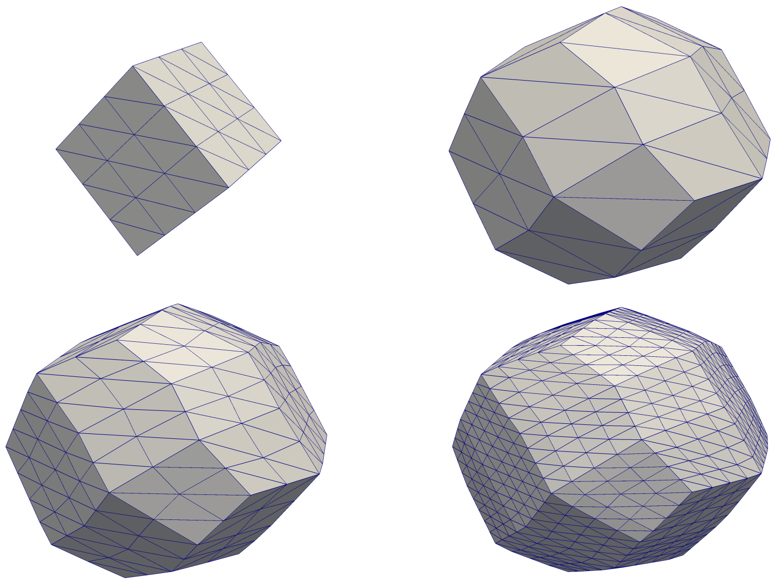

FIG. 5.5. *Numerical solutions of the problem of subsection* 5.3 *with convexity constraints: The rotational symmetry of the problem is strongly violated.*

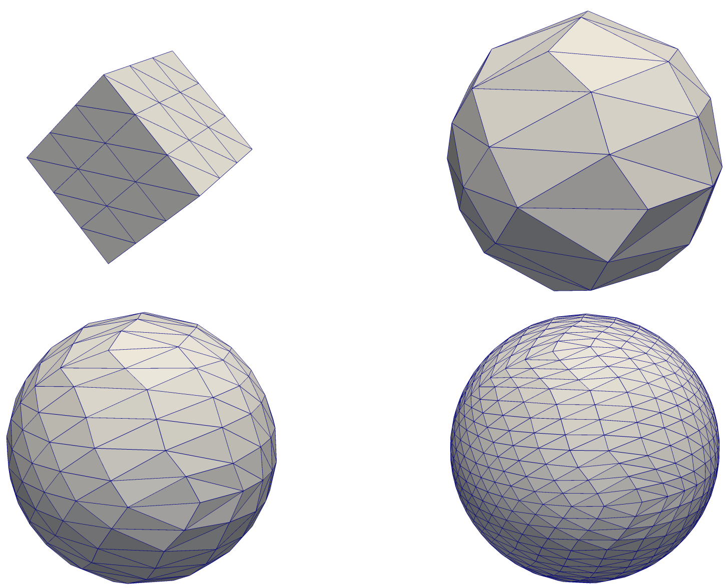

FIG. 5.6. *Numerical solutions of the problem of subsection* 5.3 *without convexity constraints: Discrete optimal shapes are nearly rotationally symmetric but not convex.*

parts" on the boundary.

Thus, the bodies in Figure 5.5 are not approximating the optimal shape, and this shows that the convergence results of section 3 do not carry over to the three-dimensional situation.

This nonconvergence phenomenon is well known for the approximation of convex functions. Indeed, in two dimensions it is not possible to approximate arbitrary convex functions by convex finite element functions of order one on, e.g., uniform refinements of a fixed grid; see Choné and Le Meur (2001). However, for functions of order at least two, there exist approximation results; see Aguilera and Morin (2009); Wachsmuth (2017).

REFERENCES

N. E. Aguilera and P. Morin (2009), *On convex functions and the finite element method*, SIAM J. Numer. Anal., 47, pp. 3139–3157, https://doi.org/10.1137/080720917.

M. S. Alnæs, J. Blechta, J. Hake, A. Johansson, B. Kehlet, A. Logg, C. Richardson, J. Ring, M. E. Rognes, and G. N. Wells (2015), *The FEniCS project version* 1.5, Arch. Numer. Softw., 3, https://doi.org/10.11588/ans.2015.100.20553.

P. R. S. Antunes and B. Bogosel (2018), *Parametric Shape Optimization Using the Support Function*, preprint, https://arxiv.org/abs/1809.00254.

H. Attouch, G. Buttazzo, and G. Michaille (2014), *Variational Analysis in Sobolev and BV Spaces: Applications to PDEs and Optimization*, 2nd ed., MOS-SIAM Ser. Optim. 17, SIAM, Philadelphia, https://doi.org/10.1137/1.9781611973488.

S. Bartels (2016), *Numerical Approximation of Partial Differential Equations*, Texts Appl. Math. 64, Springer, Cham, https://doi.org/10.1007/978-3-319-32354-1.

S. Bartels and G. Buttazzo (2019), *Numerical solution of a nonlinear eigenvalue problem arising in optimal insulation*, Interfaces Free Bound., 21, pp. 1–19.

S. Bartels and G. Wachsmuth (2018), *Numerical Approximation of Optimal Convex Shapes (Source Code)*, https://doi.org/10.5281/zenodo.2367904.

D. Bucur (2003), *Regularity of optimal convex shapes*, J. Convex Anal., 10, pp. 501–516.

D. Bucur, G. Buttazzo, and C. Nitsch (2017), *Symmetry breaking for a problem in optimal insulation*, J. Math. Pures Appl. (9), 107, pp. 451–463, https://doi.org/10.1016/j.matpur.2016.07.006.

G. Buttazzo and P. Guasoni (1997), *Shape optimization problems over classes of convex domains*, J. Convex Anal., 4, pp. 343–351.

P. Choné and H. V. J. Le Meur (2001), *Non-convergence result for conformal approximation of variational problems subject to a convexity constraint*, Numer. Funct. Anal. Optim., 22, pp. 529–547, https://doi.org/10.1081/NFA-100105306.

D. Cioranescu and F. Murat (1997), *A strange term coming from nowhere*, in Topics in the Mathematical Modelling of Composite Materials, A. Cherkaev and R. Kohn, eds., Birkhäuser Boston, Boston, pp. 45–93, https://doi.org/10.1007/978-1-4612-2032-9_4.

M. Delfour and J.-P. Zolésio (2001), *Shapes and Geometries. Analysis, Differential Calculus, and Optimization*, Adv. Des. Control 4, SIAM, Philadelphia.

M. Delfour and J.-P. Zolésio (2011), *Shapes and Geometries: Metrics, Analysis, Differential Calculus, and Optimization*, 2nd ed., Adv. Des. Control 22, SIAM, Philadelphia, https://doi.org/10.1137/1.9780898719826.

M. Dobrowolski (2006), *Angewandte Funktionalanalysis*, Masterclass, Springer, New York.

G. Dziuk (2010), *Theorie und Numerik partieller Differentialgleichungen*, Walter de Gruyter, Berlin.

T. Etling, R. Herzog, E. Loayza, and G. Wachsmuth (2020), *First and second order shape optimization based on restricted mesh deformations*, SIAM J. Sci. Comput., 42, pp. A1200–A1225, https://doi.org/10.1137/19M1241465.

T. Lachand-Robert and É. Oudet (2005), *Minimizing within convex bodies using a convex hull method*, SIAM J. Optim., 16, pp. 368–379, https://doi.org/10.1137/040608039.

A. Logg, G. N. Wells, and J. Hake (2012), *DOLFIN: A C++/Python finite element library*, in Automated Solution of Differential Equations by the Finite Element Method, A. Logg, K.-A. Mardal, and G. N. Wells, eds., Lect. Notes Comput. Sci. Engrg. 84, Springer, Berlin, Chapter 10.

J.-M. Mirebeau (2016), *Adaptive, anisotropic and hierarchical cones of discrete convex functions*, Numer. Math., 132, pp. 807–853, https://doi.org/10.1007/s00211-015-0732-7.

V. H. Schulz, M. Siebenborn, and K. Welker (2016), *Efficient PDE constrained shape optimization based on Steklov–Poincaré-type metrics*, SIAM J. Optim., 26, pp. 2800–2819, https://doi.org/10.1137/15M1029369.

B. Stellato, G. Banjac, P. Goulart, A. Bemporad, and S. Boyd (2020), *OSQP: An operator splitting solver for quadratic programs*, Math. Program. Comput., https://doi.org/10.1007/s12532-020-00179-2.

N. Van Goethem (2004), *Variational problems on classes of convex domains*, Commun. Appl. Anal., 8, pp. 353–371.

G. Wachsmuth (2017), *Conforming approximation of convex functions with the finite element method*, Numer. Math., 137, pp. 741–772, https://doi.org/10.1007/s00211-017-0884-8.

D. Yang (2009), *Shape optimization of stationary Navier-Stokes equation over classes of convex domains*, Nonlinear Anal., 71, pp. 6202–6211, https://doi.org/10.1016/j.na.2009.06.013.